Applied Catalysis B: Environmental 147 (2014) 251–263

Contents lists available at ScienceDirect

Applied Catalysis B: Environmental

journal homepage: www.elsevier.com/locate/apcatb

Chemical deactivation by phosphorous under lean hydrothermal conditions over Cu/BEA NH_3-SCR catalysts

Stanislava Andonova[a], Evgeny Vovk[b,c], Jonas Sjöblom[d], Emrah Ozensoy[b], Louise Olsson[a,*]

[a] Competence Centre for Catalysis, Chemical Engineering, Chalmers University, 412 96 Gothenburg, Sweden
[b] Chemistry Department, Bilkent University, 06800 Bilkent, Ankara, Turkey
[c] Boreskov Institute of Catalysis, 630090 Novosibirsk, Russian Federation
[d] Applied Mechanics, Chalmers University, 412 96 Gothenburg, Sweden

ARTICLE INFO

Article history:
Received 5 July 2013
Accepted 27 August 2013
Available online 1 September 2013

Keywords:
NH_3 SCR
NO_x reduction
Cu/BEA catalysts
P poisoning
Deactivation.

ABSTRACT

To obtain a better understanding of the deactivation of SCR catalysts that may be encountered due to the presence of P-containing impurities in diesel exhausts, the effects induced by P over Cu/BEA NH_3-SCR catalysts were studied as functions of the temperature of poisoning and P concentration in the feed. Cu/BEA catalysts with different Cu loadings (4 and 1.3 wt% Cu) were exposed to P by controlled evaporation of H_3PO_4 in the presence of 8% O_2 and 5% H_2O at 573 and 773 K. The reaction studies were performed by NH_3-storage/TPD, NH_3/NO oxidation and standard NH_3-SCR. In addition, a combination of several characterisation techniques (ICP–AES, BET surface area, pore size distribution, H_2-TPR and XPS) was applied to provide useful information regarding the mechanism of P deactivation. Pore condensation of H_3PO_4 in combination with pore blocking was observed. However, the measured overall deactivation was found to occur mostly by chemical deactivation reducing the number of the active Cu species and hence deteriorating the redox properties of the Cu/BEA catalysts. The process of P accumulation on the surface preferentially occurs on the "*over exchanged*" Cu active sites with the formation of phosphate species. This is likely the reason for the more severe deactivation of the 4% Cu/BEA compared to 1.3% Cu/BEA. Further, the higher NO_x reduction performance at 773 K of the P-poisoned Cu/BEA catalysts was found to originate from the lower selectivity towards NH_3 oxidation, which occurs predominately on the "over-exchanged" sites.

1. Introduction

In the last decade, the selective catalytic reduction (SCR) of nitrogen oxides (NO_x) has received significant attention due to its numerous applications to reduce NO_x emissions in the exhaust of stationary power plants, industry processes and recently also from automotive sources [1–3]. The current strategy of SCR by using NH_3, in particular for diesel-equipped vehicles [4–6] is nowadays considered as one of the most economical and effective NO_x abatement catalytic technology.

Vanadia-based catalysts ($V_2O_5/WO_3/TiO_2$) are the most commonly used and widely investigated for SCR [7]. However, the inadequate stability of these catalysts at high temperatures and at high space velocities, in combination with toxicity, shifted the focus of the investigations to another group of materials based on transition-metal ion-exchanged zeolites which offer an advantage of improved NO_x reduction performance and thermal stability in a wide temperature range. Hence, different experimental and theoretical studies [8–13] were focussed on the effect of the metal (Fe, Cu, Cr, Ce, Co and Rh) and the type of the zeolites [5,14,15] (ZSM-5, MFI, FER, BEA, SSZ-13 and SAPO-34) on the stability and the overall SCR performance of the exhaust zeolite-based catalysts. In general, Fe- and Cu-based zeolites are selected as the most active and stable SCR catalysts for NO_x reduction. In particular, it was found [16–22] that Cu-ion exchanged zeolites are characterised by superior low temperature NO_x conversion and N_2 selectivity in NH_3-SCR and direct NO decomposition.

Poisoning of the diesel exhaust catalysts caused by accumulation of impurities in the form of significant amount of oil- and fuel-derived contaminants (P, Zn, Ca, K, Na and Mg) deposited on the surface [23–30] is one of the problems that have not been totally solved with the current SCR technology. In particular, the effects induced by phosphorous (P) are one of the major problems in practical applications of the SCR catalysts due to their deactivation by P-containing impurities in biodiesel and lubricant oil additives [24]. It has been shown [31,32] that P can greatly impair

* Corresponding author. Tel.: +46 31-772 4390; fax: +46 31-772 3035.
E-mail address: louise.olsson@chalmers.se (L. Olsson).

0926-3373/$ – see front matter © 2013 Elsevier B.V. All rights reserved.
http://dx.doi.org/10.1016/j.apcatb.2013.08.041

the effectiveness of the NO_x emission control systems due to its cumulative influence over V_2O_5-WO_3/TiO_2 catalysts. Thus, even very low levels of P in the fuel may lead to deterioration over time, especially when an engine consumes a significant amount of contaminated fuel. It was shown [33,34] that the P contamination can deposit on the surface of the used automotive catalysts, in the form of different phosphate species such as a glassy/amorphous phase of Pb, Zn and Ca phosphates. In addition, it was found [35–39] that P is usually concentrated in the forward-most section of the monolithic three-way converters (TWC). A decrease in catalytic activity and changes in characteristics, such as a loss of surface area, in the front section of the TWC catalytic systems have been associated [36] with extensive phosphorus deposition. In addition, it was reported [40] that the exposure of Fe-zeolite SCR catalyst to P can lead to a loss of NO_x conversion and an increase in NH_3 slip. This was partly attributed to a loss of NH_3 storage ability due to P physical blockage.

Several studies [24,31,32,41–44] focussed on the effect of P deactivation on both model V_2O_5-TiO_2 and commercial V_2O_5-WO_3-TiO_2 catalysts. The P poisoning was investigated [42,43] using wet impregnation of the catalysts with an aqueous solution of H_3PO_4. The poisoning strength was found [42] to be relatively large at lower reaction temperatures due to the formation of different deactivating species on the surface. The decrease in SCR activity was also observed on V-based catalysts with the addition of H_3PO_4 as an extrusion binder [45]. In an attempt to study the P poisoning effect by using different approaches for chemical deactivation [24,31,32,46], it was concluded [42,43] that the real mechanism of deactivation cannot be reproduced by the wet impregnation method often employed.

Despite the numerous investigations [24,31,32,41–44] carried out with poisoned V-based catalysts, the individual effects of P as well as the influence of simultaneous poisoning in hydrothermal conditions are still not sufficiently known. There exists only a few studies in the literature [40,47,48] addressing the impact of different inorganic poisons (P, Ca, Mg, Zn, K) on the performance of Fe zeolites-based NH_3-SCR catalysts. It was found that the exposure of Fe-zeolites to P leads to a strong deactivation of the catalysts. However, a detailed knowledge about the effects related to P deactivation of Cu zeolites for NH_3-SCR catalysis is still lacking.

In the light of these findings, the efforts in the current work were focussed on studying the effects induced by P on Cu/BEA NH_3-SCR catalysts by clarifying their mechanism of deactivation under well-defined and more realistic conditions of poisoning. The monolith samples were exposed to P at different temperatures by controlled evaporation of H_3PO_4 in the presence of 5% H_2O and 8% O_2. The overall SCR operation was tested over the fresh Cu/BEA catalysts with different Cu content (4 and 1.3 wt% Cu) and compared to P-poisoned Cu/BEA samples. The reaction studies during NH_3-storage/temperature-programmed desorption (TPD), NH_3/NO oxidation and standard NH_3-SCR were performed in flow reactor experiments in the range of 423–773 K. In addition, a combination of several characterisation techniques was applied, such as inductively coupled plasma atomic spectroscopy (ICP–AES), surface area measurements, pore size distribution, H_2-temperature programmed reduction (H_2-TPR) and X-ray photoelectron spectroscopy (XPS). The analysis was directed towards clarifying the mechanism of P deactivation of the catalysts, by focussing the studies on the nature of the formed deactivating species on the surface.

2. Experimental

2.1. Catalyst preparation

Cu/BEA catalysts with different Cu content (1.3 and 4 wt% Cu) were prepared following the procedure of ion exchange of BEA zeolite (SiO_2/Al_2O_3 = 38, Zeolyst International) with $NaNO_3$ (Merck) and then with $Cu(CH_3COO)_2$ (Merck). In the first step, the Na-form of BEA samples was prepared by exchanging 50 g of the zeolite in a solution of $NaNO_3$ by varying the concentration of the solution (21.6 and 108 mM $NaNO_3$, respectively). The exchange was carried out by agitating the slurry at room temperature for 1 h, with the initial pH adjusted to 6.6 and kept constant using NH_4OH. The solid was then filtered and washed until the neutral pH of the filtrate was reached. The above process including the ion-exchange, filtering and washing was repeated two times. In the second stage, the Na-form of BEA samples dried at 353 K for 12 h, were used for the next step of Cu ion exchange with $Cu(CH_3COO)_2$ by varying the Cu precursor concentration (2.2 and 11 mM $Cu(CH_3COO)_2$, respectively). The exchange was carried out by agitating the slurry at room temperature for 1 h, with the initial pH adjusted to 6.0 and kept constant during the stirring. After filtration and washing the above process of Cu ion-exchange was repeated two more times to give a total of three exchanges. Finally, the resulting powder was dried at 353 K for 12 h and calcined at 723 K for 3 h.

The calcined powder catalysts were used to coat cordierite monoliths. The monoliths were cut from a commercial honeycomb cordierite structure (length = 20 mm, diameter = 22 mm and cell density of 400 cpsi) and heated to 773 K for 2 h. A solid phase of 5 wt% boehmite (Disperal D, Sasol, GmbH) dissolved in a slurry mixture consisting of the liquid phase (distilled water/ethanol = 50/50) was first used for the impregnation of the calcined monoliths in order to enhance the attachment of the ion exchanged catalyst. The alumina-coated monoliths were calcined at 773 K for 2 h. Then, the procedure consisted of immersing the monoliths into a slurry composed of a liquid phase of equal amounts of distilled water and ethanol and a solid phase of 5 wt% boehmite and 95 wt% catalyst. The solid in the slurry was 20% w/w. The procedure of the immersion, blowing away the excess slurry, drying (363 K for 2 min) and heating (823 K for 2 min) in air was repeated several times until the monolith was coated with the desired amount of washcoat (~700 mg). Finally, the wash-coated monoliths were calcined at 773 K for 2 h.

2.2. P exposure of Cu/BEA catalysts in lean hydrothermal conditions

The P poisoning of the Cu/BEA monolith samples was performed by using the experimental set-up which has been described in detail elsewhere [49,50]. The monolith catalyst was inserted in the middle of the heated zone of a horizontal quartz tube reactor, which was equipped with an insulated heating wire controlled by Eurotherm temperature-controller. The temperature was measured with a thermocouple positioned about 10 mm in front of the monolith and a second one placed in the centre of the monolith. To simulate P poisoning in lean hydrothermal conditions, an aqueous solution of H_3PO_4 in the form of steam was fed into the quartz reactor (by using a controlled evaporation and mixing via a Bronkhorst system) in the presence of 5% H_2O, 8% O_2 and Ar. The total gas flow rate was held constant at 3500 ml min^{-1}, giving a space velocity of 30,300 h^{-1}, based on monolith volume. The resulting mixture was then passed over the monolith samples. The procedure was developed to compare the effects of poisoning at two different temperatures at 573 and 773 K, while the duration of the exposure (4.4 h) was kept constant. The monoliths were first exposed at 573 K to 50 ppm P and then to 100 ppm P by increasing the amount of H_3PO_4 in the feed. In a similar way, the P poisoning at the higher temperature (773 K) was carried out by using a new monolith sample. To determine the effect of changing the P concentration and the temperature of poisoning, the activity measurements (described below) were performed over the fresh and P-poisoned catalysts after each step of P exposure. To prevent the formation of $(NH_4)_3PO_4$, after the procedure

of P poisoning, an extensive cleaning of the reactor was carried out before starting the activity measurements over the poisoned catalysts. All lines were heated and maintained at temperatures above 423 K to prevent water and H_3PO_4 condensation.

2.3. Catalyst characterisation

The elemental analysis of the fresh and P-poisoned catalysts (crushed monoliths) was determined by an ICP–AES after $LiBO_2$-fusion and acid digestion of the samples.

The textural properties of the monolith samples previously degassed at 523 K for 3 h were measured based on N_2 adsorption–desorption isotherms using a Micromeritics ASAP 2000 apparatus. BET surface area (S_{BET}) and total pore volume (V_{pores}) were calculated using the BET and Barret–Joyner–Halenda (BJH) method, respectively. Pore size distributions were obtained by applying the BJH model to N_2 desorption data.

The experimental set-up used for the H_2-TPR experiments comprises a vertical quartz tube reactor mounted in an electric furnace, part of the assembly of the heat-flux differential scanning calorimetry (Setaram Sensys DSC) instrument. The gas flow into the reactor was controlled by using a system of Bronkhorst mass flow controllers. Prior to each measurement, the catalyst (approximately 0.1 g of powder of crushed monolith samples placed on the sintered bed of the quartz tube) was first treated with a mixture of 5% O_2 in Ar at 773 K for 2 h. The temperature was then decreased to 323 K under the same gas environment. After flushing with only Ar at 323 K for 30 min, a flow of 1% H_2/Ar (20 ml min^{-1}) was passed through the sample at 323 K for 20 min and then the temperature in the presence of 1% H_2/Ar was raised at a rate of 10 K min^{-1} up to 1073 K. The effluent from the reactor was monitored using a Hiden HPR 20 quadrupole mass spectrometer (MS) equipped with a capillary probe connected directly to the exit of the reactor. The analysis was performed by recording the MS signals with mass to charge ratio (m/e) equal to 2, 18, 20 and 32 in pressure versus time mode.

XPS data were recorded with a Thermofisher K-Alpha spectrometer using non-monochromatic Al Kα X-ray irradiation. The powder samples were affixed on a Cu-based electrically conducting tape before the XPS analysis. An e-beam flood gun was used for charge compensation during the spectral acquisition. The binding energies (BE) of all XP spectra were calibrated by utilising the reference C1s signal located at 284.6 eV and the XP intensities were normalised using the intensity of the O1s signal of each XP spectrum.

2.4. Flow reactor measurements with monolith catalysts

The reaction studies on the monolith catalysts were performed on the experimental set-up described above for the P poisoning experiments. Approximately 700 mg catalyst washcoated on the monolith was used in each experiment yielding a space velocity of 30,300 h^{-1}, based on monolith volume. The total gas flow was held constant at 3500 ml min^{-1} and controlled by a system of Bronkhorst mass flow controllers. The water in the form of steam was introduced into the reactor by using a controlled evaporation and Bronkhorst mixing system. The monoliths were wrapped with quartz wool to ensure that no gas slipped around the sample. The outlet gas composition from the reactor flow was monitored and analysed on-line with respect to NO, NO_2, N_2O, NH_3, and H_2O content by using MKS MultiGas 2030 HS FTIR spectrometer. To maintain a constant catalytic behaviour over the course of the study, the catalysts were degreened by increasing the temperature to 773 K in Ar; then the samples were cleaned/conditioned with 8% O_2 in Ar for 15 min and then the catalysts were treated with a gas mixture of 400 ppm NO + 400 ppm NH_3 + 8% O_2 + 5% H_2O and balancing amounts of Ar for 30 min. Prior to each experiment, the catalysts were pre-treated at 773 K in Ar and 8% O_2 for 15 min.

Table 1
Flow reactor measurements performed in a predefined sequence of steps over the fresh and P-poisoned Cu/BEA monolith catalysts.

Samples	Reaction studies
Fresh	1. NH_3 storage/TPD
	2. NH_3-SCR
	3. NO oxidation
	4. NH_3 oxidation
P–poisoned	1. NH_3-SCR up to 573 K
	2. NO oxidation up to 573 K
	3. NH_3 oxidation up to 773 K
	4. NH_3-SCR up to 773 K
	5. NH_3 storage/TPD
	6. NO oxidation up to 773 K
	7. NH_3 oxidation up to 773 K (rep.)

The following experiments over the fresh and P-poisoned catalysts were carried out:

(a) *NH_3 storage tests and TPD in the presence of H_2O* – The catalysts were initially exposed to 400 ppm NH_3 in the presence of 5% H_2O for 40 min at 423 K. After flushing with Ar + 5% H_2O for 30 min, the temperature was raised to 773 K with a ramp speed of 10 K min^{-1}. The outlet NH_3 concentration was monitored as a function of time and then converted to the cumulative NH_3 stored during the uptake period as a percentage of the NH_3 fed, by integrating the area included between the inlet NH_3 and the outlet NH_3 concentration curve.

(b) *Flow reactor studies* – The activity measurements were carried out at 423, 473, 523, 573, 673 and 773 K. The results for each temperature were obtained after the system had reached a steady-state and then the reactor temperature was increased to the next target test reaction temperature. In this way, the experiments were conducted within 423–773 K while the reaction mixture was continuously fed during the whole temperature range. The experiments of NH_3 or NO oxidation under lean conditions were performed with an inlet gas mixture consisting of 8% O_2, 400 ppm NH_3 (or 400 ppm NO), 5% H_2O and a balance of Ar. The reaction studies of SCR with NH_3 were performed with an inlet gas mixture consisting of 8% O_2, 400 ppm NH_3, 400 ppm NO, 5% H_2O and a balance of Ar.

For comparison of the results, the reaction studies prior to and after P poisoning were performed in a predefined sequence of experiments, presented in Table 1. In the first stage, the activity measurements of NH_3 storage/TPD, standard NH_3-SCR, NO and NH_3 oxidation were conducted over the fresh degreened catalysts. Then, the samples were subjected to P poisoning with 50/100 ppm P at 573 K, followed by activity measurements between each step of exposure with the different concentration of H_3PO_4. In a similar way, the experiments of P poisoning at higher temperatures (773 K) were performed by using another fresh monolith sample. Due to the possibility of formation of loosely bound P species which can easily be removed by heating the sample at high temperatures, the P-poisoned samples were first tested in standard NH_3-SCR and NO oxidation up to 573 K (Table 1). Then, the experiments were repeated at various temperatures within 423–773 K.

To evaluate the overall SCR performance of the catalysts, the outlet concentration curves were used to determine the activity per Cu site, expressed as a ratio of the amount (kmol) of NO_x reduced or NH_3 converted species per mol of Cu sites per second. The results for each temperature were obtained after the system had reached a steady-state. The outlet NH_3 and NO_x concentrations during NH_3 oxidation and NH_3-SCR were monitored as a function of time and then converted to NO_x and NH_3 reacted, according to Eq. (1):

$$[NO_x(NH_3)]^{reacted} = [NO(NH_3)]^{in} - [NO_x(NH_3)]^{out} \quad (1)$$

(NO^{in}) and (NH_3^{in}) are the NO and NH_3 concentrations at the reactor inlet; (NO_x^{out}) and (NH_3^{out}) are total NO_x and NH_3 concentrations at the reactor outlet, respectively.

The amount of reacted NO_x (or NH_3) per Cu site, defined as the number of NO_x (NH_3) molecules (kmol) converted per mole of Cu per second (over the fresh and P-poisoned catalysts) was calculated by using Eq. (2), as:

$$\text{kmol } NO_x(NH_3)^{\text{reacted}} \text{per mol Cu} = \frac{\left[NO_x^{\text{reacted}}(NH_3^{\text{reacted}})(\text{ppm}\times\text{s})\times \text{TF}(\text{ml}\times\text{min}^{-1})\times 10^{-6}(\text{ppm}^{-1})\right]}{\left[22414(\text{ml}\times\text{kmol}^{-1})\times 60(\text{s}\times\text{min}^{-1})\times m_{\text{washcoat}}(\text{g})\times \text{Cu}(\text{mol}\times\text{g}_{\text{cat}}^{-1})\right]}\times 100 \quad (2)$$

where, TF (ml min^{-1}) is the gas flow rate (3500 ml min^{-1}) and m_{washcoat} (g) is the mass of the washcoat on the monolith.

To estimate the degree of deactivation of the catalysts, the reduction of NO_x conversion in the reaction of NH_3-SCR due to P poisoning was estimated by using Eq. (3):

$$\text{Reduction of } NO_x \text{after poisoning} = \frac{\left[NO_x^{\text{reacted}}(\text{kmol})\right]^{\text{Fresh}} - \left[NO_x^{\text{reacted}}(\text{kmol})\right]^{\text{Aged}}}{\left[NO_x^{\text{reacted}}(\text{kmol})\right]^{\text{Fresh}}}\times 100 \quad (3)$$

$\left[NO_x^{\text{reacted}}\right]^{\text{Fresh}}$ and $\left[NO_x^{\text{reacted}}\right]^{\text{Aged}}$ are the amounts (kmol) of total NO_x converted per mol of Cu sites over the fresh and P-poisoned catalysts per second.

In a similar way, the decrease in the NH_3 conversion during NH_3-SCR was calculated according to Eq. (3), by using the amounts (kmol) of NH_3 converted over the fresh and P-poisoned catalysts.

3. Results and discussion

3.1. Chemical composition and textural characteristics of the catalysts

3.1.1. ICP, BET surface area and pore size distribution

The ICP–AES analysis of the Cu/BEA catalysts was carried out to quantify the amount of Cu, Al and Si on all of the powder samples before their washcoating, while P analysis was only performed for P-poisoned monolith samples. The results are listed in Table 2. The composition-dependent changes of the textural properties (S_{BET}, V_{pore}) of the fresh and P-poisoned Cu/BEA catalysts with different Cu loadings are also summarised in Table 2. In addition, BJH pore size distributions for different monoliths are also presented in Fig. 1.

In the case of BEA ion-exchanged samples with different Cu content, the ICP–AES analysis indicated that the synthesis which was controlled by changing the concentration of Cu in the ion-exchange solution has resulted in Cu/BEA catalysts with Cu contents of 4.0 and 1.3 wt% Cu. In our previous study [10], elemental analysis of the powder catalysts before their washcoating showed that the Cu ion exchange level in 4Cu/BEA sample is close to 88%. This sample can be regarded as an over-exchanged system compared to the 1.3Cu/BEA sample with a lower Cu content and a lower Cu exchange level of ~30%. This is also in agreement with other studies [12,51] in the literature, where the Cu/BEA catalysts have been considered as "*over-exchanged*" when the exchanged level based on the Cu/Al ratio is more than 50%. It is worth mentioning that, the current ICP–AES analysis showed that Si/Al ratio typically remains similar for the analysed samples, while trace amounts of P (i.e. comparable to the instrumental detection limit) were also observed on the fresh samples.

Conversely, P content to the P-poisoned 4Cu/BEA samples was noticeably higher than the fresh catalysts, indicating that the exposure of the monolith samples with H_3PO_4 in lean hydrothermal conditions has resulted to the accumulation of P in the samples. The P content detected for both 4Cu/BEA samples exposed to H_3PO_4 at 573 K (P1) and 773 K (P2) was 11.3 and 11.9%, respectively. On the other hand, on the 1.3Cu/BEA sample with the lower Cu content, which was poisoned under identical conditions as for the 4Cu/BEA catalyst (i.e. 573 K (P1), P accumulation was observed to be only 1.4%.

The textural characteristics of the fresh, non-poisoned Cu/BEA catalysts synthesised with different Cu content showed that the ion-exchanging of the zeolite with the higher concentration of Cu (i.e. 4.0 wt% Cu) resulted in a slight decrease of the total surface area and the pore volume compared to the sample with the lower Cu content (i.e. 1.3 wt% Cu). Such behaviour is expected and indicates that the incorporation of Cu ions occurs through substitution of existing Na^+ cations at the ion-exchange sites, and proceeds without significant occlusion of pore network. On the other hand, a considerable difference in the textural characteristics of the P-poisoned Cu/BEA catalysts was observed (Table 2). The poisoning by P was found to have a significant effect on the specific surface area and pore volume of the catalysts which were diminished compared to the fresh monolith samples. These results are also consistent with the data presented in Fig. 1, where it can be seen that the deposition of H_3PO_4 produced a significant change in the pore size distribution for the monoliths exposed to P. It is visible that the fresh, non-poisoned monolith samples have a higher pore volume and the pore size distribution plot contains two peaks, around 3.6 and 5.1 nm. The smaller pores are attributed to intercrystalline distance within the aggregates whereas the bigger pores are likely to originate from the inter-aggregate distance. It was found that the pores with larger diameter of the bimodal mesoporous structure were partially filled after P poisoning of the 4Cu/BEA catalysts, indicating the occurrence of physical deactivation most likely due to pore blocking and condensation. According to these results, it was suggested that the deposited P may act as impurities blocking the pores. Therefore, further information regarding the possibility for chemical deactivation of the catalysts was obtained by H_2-TPR of the samples.

3.1.2. H_2-TPR

The redox behaviour of the Cu/BEA catalysts after P poisoning was studied by TPR analysis performed by recording the H_2 consumed as function of the temperature in the range of 323–1073 K. Fig. 2 presents the H_2-TPR profiles for fresh 1.3Cu/BEA and 4Cu/BEA samples as well as similar measurements for the same samples poisoned with P at 573 and 773 K.

The reduction signal observed in the TPR profile of the 4Cu/BEA sample reveals three major features at 454, 520 and 578 K. The H_2-TPR of Cu/BEA catalysts with different Cu loadings has been thoroughly discussed in various former studies [12,52–54]. Based on these reports, the first prominent signal at 454 K in the TPR of the 4Cu/BEA sample was attributed to the reduction of Cu^{2+} ions in Cu—O—Cu structures, which can be formed at high Cu ion exchange levels. It was reported [12,52–54] that these dimeric Cu species observed for large Cu-loadings contain bridging oxygen atoms that can react with H_2 at comparably low temperatures than isolated Cu-sites. This is also in good agreement with the H_2-TPR curve of 1.3Cu/BEA catalyst with the lower Cu content, where the temperature maxima shift to higher temperatures (at about 671 and 839 K) with decreasing the Cu content. Significantly lower temperature maxima are observed for the 4Cu/BEA catalyst as compared to the 1.3Cu/BEA system, which clearly shows that the reducibility of the over-exchanged 4Cu/BEA sample is substantially higher than that of the 1.3Cu/BEA catalyst. This can be associated with the smaller population of isolated Cu-sites in the case of 4Cu/BEA sample which

Table 2
Elemental composition, specific surface area (S_{BET}) and total pore volume (V_{pores}) of the fresh and P-poisoned Cu/BEA monolith catalysts.

Monolith sample	Temperature of P poisoning (K)	Elemental analysis (%)				S_{BET} ($m^2\,g^{-1}$)	V_p ($cm^3\,g^{-1}$)
		Cu [c]	P	Al [c]	Si [c]		
4Cu/BEA [a]	–	4	1.1	1.9	42	146	0.105
4Cu/BEA–P1 [b]	573	4	11.3	1.9	42	116	0.0892
4Cu/BEA– P2 [b]	773	4	11.9	1.9	42	109	0.0806
1.3Cu/BEA [a]	–	1.3	0.92	1.9	41.3	154	0.107
1.3Cu/BEA–P1	573	1.3	1.4	1.9	41.3	141	0.090

[a] Fresh, non poisoned sample.
[b] P1/P2–P poisoned samples after exposure of the monoliths with P at 573 and 773 K, respectively.
[c] Cu, Al and Si content in the samples (wt%) was determined by ICP analysis of Cu/BEA powder catalysts without the monolith and the binder.

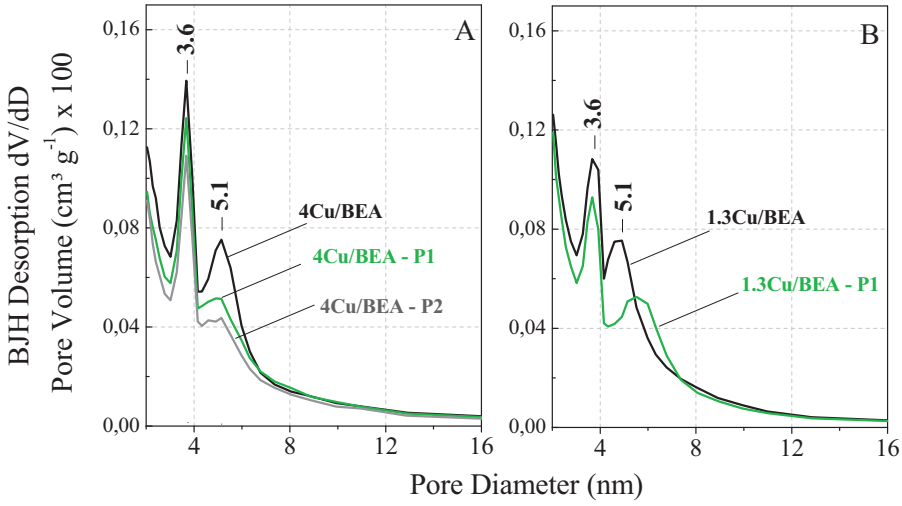

Fig. 1. BJH pore size distribution of the fresh and P-poisoned at 573 K (P1) and 773 K (P2) Cu/BEA monoliths samples with different Cu content (4 and 1.3 wt% Cu): 4Cu/BEA–Fresh/P1/P2 (A) and 1.3Cu/BEA–Fresh/P1 (B).

requires a less facile [12,52–54], two-step reduction mechanism [53] in which isolated Cu^{2+} ions are initially reduced to the Cu^{+} intermediate and then to metallic Cu species.

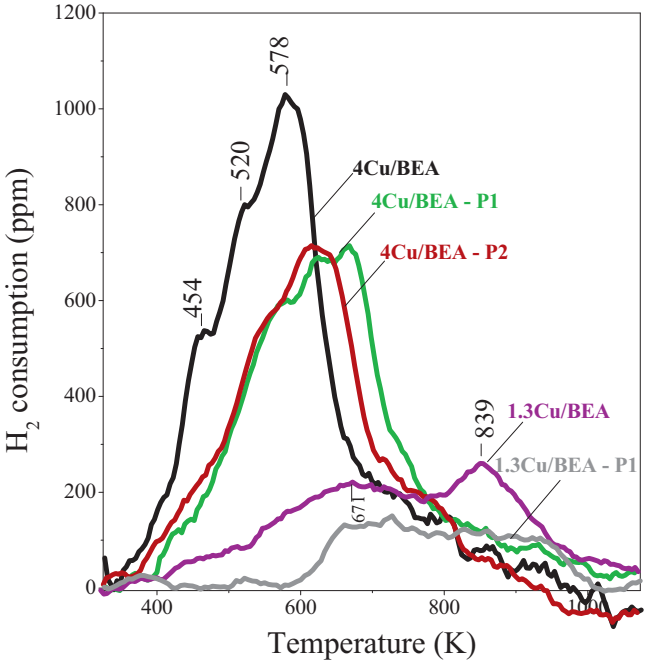

Fig. 2. H_2-TPR of the fresh and P-poisoned at 573 K (P1) and 773 K (P2) Cu/BEA monoliths samples with different Cu content (4 and 1.3 wt% Cu).

The TPR signals at 520 and at 578 K for the 4Cu/BEA sample can also be interpreted via two different explanations based on the former studies [12,52–55] in the literature. It was shown in Ref. [12,52–54] that these H_2 consumption peaks could be related to the two-step reduction of Cu^{2+} to Cu^{+} (i.e. 520 K signal) followed by Cu^{+} to Cu^{0} (i.e. 578 K signal). Alternatively, by referring to another experimental study [55], it can also be argued that these two different TPR peaks are indicative of the reduction of two different types of Cu^{2+} sites into Cu^{+} species.

Fig. 2 clearly shows that the P-poisoning results in significant changes in the TPR profiles. The 4Cu/BEA catalysts after P poisoning are characterised with significantly higher reduction temperatures compared to that of the fresh 4Cu/BEA. Moreover, this effect is more discernible for the catalyst exposed to P at 573 K. In addition, the TPR signal intensities for P-poisoned samples decreased dramatically in comparison with the fresh catalysts. The fraction of the reduced Cu sites (in $mol\,g^{-1}$ cat) and the total integral H_2 consumption signals obtained from the H_2-TPR results are presented in Table 3. These results showed that the total H_2 consumption ($6.16 \times 10^{-4}\,mol\,g^{-1}$ cat) of the fresh 4Cu/BEA catalyst closely matches the Cu loading in the same catalyst ($6.30 \times 10^{-4}\,mol\,g^{-1}$ cat)). Such behaviour suggests that almost 100% of the existing Cu^{2+} sites were reduced during the TPR experiments. On the other hand, TPR data for the poisoned samples reveal that only 76–78% of the Cu sites existing on the fresh catalysts remained available for reduction after P poisoning. In other words, the fraction of the reduced Cu species over P-poisoned 4Cu/BEA catalysts is about 20% lower in comparison to that of the fresh sample, indicating the attenuation of the number of available Cu sites for reduction. In a similar way, the total amount of H_2 consumption ($1.97 \times 10^{-4}\,mol\,g^{-1}$ cat) for the fresh 1.3Cu/BEA catalyst closely

Table 3
Calculated parameters via H_2-TPR and surface compositions of the analysed fresh and P-poisoned Cu/BEA monolith samples via XPS analyses.

Samples	H_2 - TPR		XPS			
	Total H_2 consumed (mol g^{-1} cat) x 10^{-4}	Total Cu reduced (%)[a]	Cu(II)/(Cu(I) + Cu(0))[b]	Cu(II)%[c]	Cu/Si[d]	P/Si[d]
4Cu/BEA	6.16	97.8	1.6	62	0.04	–
4Cu/BEA–P1	4.83	76.7	3.3	77	0.05	0.03
4Cu/BEA–P2	4.95	78.7	3.3	77	0.06	0.03
1.3Cu/BEA	1.97	96.4	1.0	50	0.01	–
1.3Cu/BEA–P1	1.73	84.3	0.3	25	0.01	–

[a] Percent of total Cu reduced was calculated based on the total amount of Cu (mol g^{-1} cat) in the samples and the total integral H_2 consumption during H_2-TPR.
[b] Relative abundance of Cu(II) species with respect to the abundance of all Cu(I) and Cu(0) species
[c] Percent abundance of Cu(II) species with respect to the total abundance of Cu(II), Cu(I) and Cu(0) species
[d] Relative surface atomic ratios obtained from the corresponding integrated XPS signals and atomic sensitivity factors (ASF)

coincides with the Cu content (2.05×10^{-4} mol g^{-1} cat) in this sample. Although the effect is much more suppressed in comparison to the sample with the higher Cu loading, the total H_2 consumption of the 1.3Cu/BEA–P1 sample decreased by ~10% after P poisoning.

In the light of these observations, it can be suggested that the poisoning by P follows both physical and chemical deactivation pathways. It is evident that the exposure of the monoliths with P chemically deactivates the Cu/BEA catalysts by decreasing the number of the active Cu species and hence hindering their redox capabilities. Furthermore, P poisoning has a considerable effect on the metal zeolite interaction by producing Cu species which are strongly bonded to the framework oxygen resulting in a higher temperature of reduction. Moreover, it is also likely that P-poisoning may also lead to the formation of Cu- phosphate species. This is particularly likely as the P source used in the poisoning experiments was H_3PO_4, which can readily generate phosphates upon its deposition on the catalyst surface. Therefore, further information regarding the nature of the P-containing species generated after the poisoning process was obtained via XPS experiments which will be discussed in Section 3.1.3.

3.1.3. XPS

The $Cu2p_{3/2}$ and P2p XP spectra of the fresh and P-poisoned Cu/BEA samples are presented in Fig. 3. This set of data corresponds to triturated powder samples which include a mixture of washcoat together with the monolith. It is worth mentioning that XPS analyses were also performed over the same set of catalyst samples using different sampling techniques (e.g. by scrapping the washcoat from the monolith walls or by directly analysing the interior walls of the monolith by breaking the monolith channels), which revealed similar results as compared to the triturated samples discussed below. It is known [56] that the shake-up satellite positioned at c.a. 943 eV in the $Cu2p_{3/2}$ spectra is an indication of the presence of Cu(II) species. Two discernible features of the main $Cu2p_{3/2}$ signal seen in Fig. 3A at 934.7 and 933.6 eV can be attributed to Cu(II) and Cu(I)/Cu(0) species, respectively. The Cu(I) state can be qualitatively differentiated from Cu(0) signal from the corresponding LMM Auger signal, [56] however due to low Cu content of the analysed samples, acquisition of a reliable LMM Auger signal was not feasible in the current XPS measurements. Thus, the latter $Cu2p_{3/2}$ signal at 933.6 eV is tentatively assigned to Cu(I) and/or Cu(0) species. Although the current XPS results do not provide a direct evidence for ruling out the existence of Cu(0) species, presumably existence of such a highly reduced Cu state seems rather unlikely. Comparison of the spectra corresponding to the fresh and P-poisoned 4Cu/BEA catalysts presented in Fig. 3A indicates that the Cu $2p_{3/2}$ peaks for both 4Cu/BEA–P1(P2) samples after P poisoning show significant asymmetry with respect to that of the fresh catalytic system. It is visible that the $Cu2p_{3/2}$ spectra of the 4Cu/BEA–P1(P2) catalysts consist of strongly pronounced shoulder on the higher binder energy side at 934.7 eV of the main peak at 933.6 eV while the $Cu2p_{3/2}$ peak of the fresh 4Cu/BEA sample looks more symmetric. Thus, it is presumable that the presence of P brings about a visible variation in the populations of Cu species with different oxidation states. Therefore, the relative amount of Cu(II) versus Cu(I)/Cu(0) species was estimated with the help of the shake-up satellite signal, since Cu(I) and Cu(0) species do not reveal this particular satellite signal. It is possible to calculate Cu(II)/(Cu(0) + Cu(I)) ratio by comparing integrated areas of the shake-up satellite and the main $Cu2p_{3/2}$ signals. This method is described comprehensively in the work of Biesinger et al. [56]. As described in this former report [56], for the calculation of Cu(II)/(Cu(0) + Cu(I)) ratio, one needs to know the ratio of the integrated peak areas of the main Cu2p signal located at c.a. 933–935 eV and the satellite feature at c.a. 943 eV for a pure CuO reference material. In our calculations, we used a value of 1.9 for this purpose, which has been reported by Biesinger et al. [56]. The results obtained via this analysis are presented in Table 3.

XPS data corresponding to both fresh and P-poisoned 4Cu/BEA catalysts indicate the increased fraction of Cu(II) in the P-poisoned samples with respect to the fresh system. It was found that the fraction of the Cu(II) after P poisoning of the 4Cu/BEA catalyst is about 15% higher in comparison to that of the P-free sample.

On the other hand, the data for the samples with 1.3 wt% Cu loading demonstrate sufficiently lower Cu(II)% content in comparison to the samples with 4 wt% Cu loading, particularly for P-poisoned samples. It is important to note that Cu (II) species are prone to reduction upon exposure to X-rays. Reduction of Cu(II) species due to X-ray irradiation has been reported in former studies [57,58] associated with Cu-based catalytic systems. In the current XPS measurements, we did not particularly focus on the X-ray induced reduction of the analysed samples. However, it is worth mentioning that when the Cu2p XP spectra obtained after 15 min of X-ray exposure were compared with the XP spectra obtained from identical set of samples after longer (i.e. 2 h) X-ray exposure; no apparent differences were detected between these two set of data. On the other hand, this observation does not exclude the possibility of X-ray induced reduction of Cu(II) sites which could have taken place in the very first 15 min of the XPS analysis. The data from the H_2-TPR shows that 98 and 96% of the copper in the 4Cu/BEA and 1.3Cu/BEA were in the form of Cu(II) (calculation based on Cu(II) to Cu(0) in the TPR), respectively. The XPS data show significantly less Cu(II) and the reason could be reduction of the copper by the beam in the first minutes of the experiments, as seen by Wilken et al. [57]. If this is the case, XPS gives important information about the reducibility of the copper between the different samples. The XPS reveal that the copper species in 4Cu/BEA are more difficult to reduce after phosphorous exposure, which is in line with the higher temperature for reduction in the TPR. This is not seen for the low loading sample, but on the other hand the loading is very low, making this analysis more difficult.

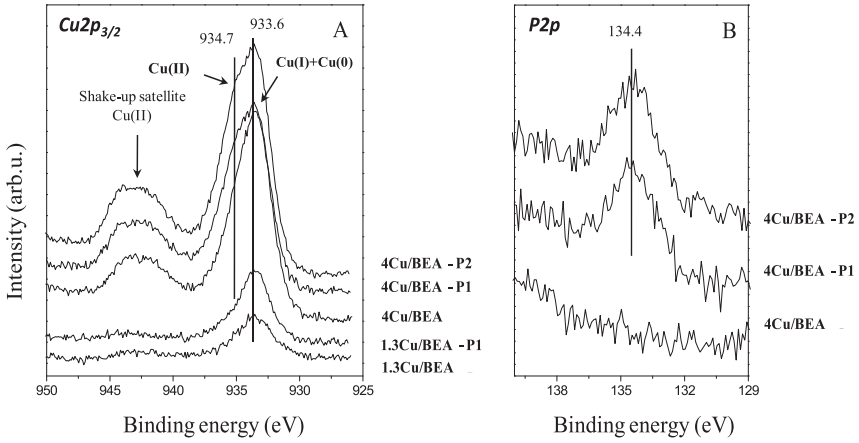

Fig. 3. Cu2p (A) and P2p (B) XP spectra of the fresh and P-poisoned at 573 K (P1) and 773 K (P2) Cu/BEA monoliths samples with different Cu content (4 and 1.3 wt% Cu).

We have also analysed the P2p signal in the XP spectra (Fig. 3B) for the samples given in Table 3. Phosphorous could only be detected for the P-poisoned 4Cu/BEA samples with a higher Cu loading, while P2p signal was below the instrumental detection limit for the catalyst samples with the lower Cu content (i.e. 1.3Cu/BEA). This observation suggests that Cu sites may be functioning as PO_x anchoring sites in the Cu/BEA catalytic system. The P2p XP signals given in Fig. 3B reveal a broad feature located at 134.4 eV, which can be associated with phosphate, metaphosphate [59,60], and/or dihydrogen phosphate [61] functionalities, as all of these species reveal relatively similar P2p binding energy values for different metal cations.

Based on the XPS results combined with the H_2-TPR, it is apparent that PO_x species (most likely in the form of phosphates) strongly interact with active Cu sites on the catalysts, leaving a smaller number of accessible Cu sites available for reduction via H_2-TPR.

3.2. Flow reactor measurements

Further information regarding the effects induced by chemical deactivation of Cu/BEA catalysts with P was obtained via flow reactor measurements on the wash-coated monolith samples.

3.2.1. NH_3-storage and TPD

In Fig. 4, time-dependent NH_3 uptake (at 423 K) and TPD (423–773 K) measurements in the presence of 5% H_2O are presented.

It is visible in Fig. 4A that the presence of P in the 4Cu/BEA sample has a significant effect on the breakthrough profile of ammonia and on the corresponding NH_3 uptake behaviour of the system poisoned with 50 ppm P and then with 100 ppm P at 573 K. The NH_3 signal during the exposure period is more significantly delayed for the fresh 4Cu/BEA in comparison to the 4Cu/BEA–P1 sample. On the other hand, the NH_3 adsorption experiments performed over the 4Cu/BEA–P2 catalysts (Fig. 4B) showed NH_3 uptake behaviour similar to that of the fresh 4Cu/BEA with very small deviations in the NH_3 concentration profiles. Such a situation is also valid for the 1.3Cu/BEA catalyst with lower Cu content presented in Fig. 4C.

The analysis of the TPD data in Fig. 4 for the poisoned samples shows similar trends, without any significant temperature shift in the desorption maxima. However, the NH_3 signals in the TPD of the P- poisoned 4Cu/BEA catalysts reveal lower desorption intensities (Fig. 4A). This effect is much more strongly pronounced in the TPD profiles of the 4Cu/BEA catalysts P poisoned at 573 K with 50 and 100 ppm P. Based on the data presented Fig. 4D, it can be seen that the extent of P poisoning increases monotonically with the increasing amount of H_3PO_4 in the feed.

The effect of the P poisoning at 773 K on the NH_3 storage ability, particularly in the case of the 4Cu/BEA–P2 (Fig. 4B) is limited in comparison to that for the 4Cu/BEA–P1 sample. This behaviour can be explained by considering the proposed mechanism of P deposition in the study [31] investigating deactivation of V-based commercial SCR catalysts by H_3PO_4. It was shown in this former study that H_3PO_4 molecules start condensation reactions forming polyphosphoric acids which can be deposited on the surface at temperatures lower than 773 K. Once deposited on the catalyst outer surface, these species were found [31] to have high mobility and ability to penetrate and even be trapped into the walls by capillary forces.

In the light of these findings, it can be suggested that P poisoning of the 4Cu/BEA catalysts at 773 K hinders the chemical deactivation of the samples due to inefficient condensation/polymerisation reactions of the deposited H_3PO_4 at elevated temperatures, resulting in loosely bound PO_x species. It is worth mentioning that XPS and ICP–AES results for the 4Cu/BEA–P1/P2 samples given in Tables 2 and 3 reveal similar P surface atomic ratios for these two samples. This observation points to the fact that chemical nature of the poisoning PO_x species could have a more central role than the sole surface coverages of such functionalities. Along these lines, although the chemical structures of the poisoning PO_x species are likely to be different on the 4Cu/BEA–P1 and 4Cu/BEA–P2 samples, such structural differences seem to be elusive to capture via XPS as these two samples yield very similar P2p XP spectra (Fig. 3B).

The NH_3 uptake behaviour of the fresh and P-poisoned at 573 K 1.3Cu/BEA catalyst is presented in Fig. 4C. Despite the lower temperature of P exposure of the monolith sample at 573 K, the results showed an NH_3 storage behaviour, which is similar to that of the fresh catalyst. The amount of stored NH_3 on 1.3Cu/BEA gradually decreases with increasing the P concentration. However, the poisoning process is much less pronounced compared to that for the "*over exchanged*" 4Cu/BEA sample with higher Cu content. Thus, it can be argued that the process of P accumulation on the surface has occurred preferentially on the so called "*over exchanged*" Cu active sites (which are abundant on the 4Cu/BEA sample). This is in agreement with the current ICP–AES data which showed that the P content is only 1.4% P, although the conditions of poisoning were identical for the 4Cu/BEA–P1 catalyst. In addition, the H_2-TPR data showed no significant changes in the redox-properties of the

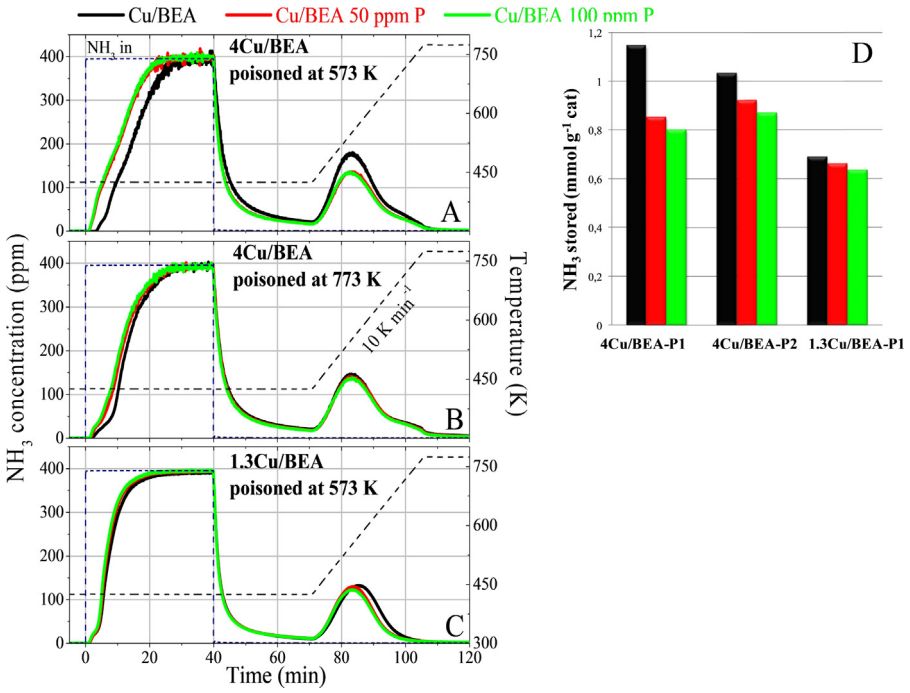

Fig. 4. Evolution of NH_3concentration as function of the time during NH_3 uptake (at 423 K) and TPD (423–773 K) in the presence of 5% H_2O over the fresh and P-poisoned at 573 K (P1) and 773 K (P2) Cu/BEA catalysts after exposure of the samples with 50 and 100 ppm P: 4Cu/BEA (A and B) and 1.3Cu/BEA (C). The inset (D) presents the estimated amounts of NH_3 stored on the surface (mmol) per gram catalysts as function of the temperature of P poisoning.

P-poisoned 1.3Cu/BEA catalyst compared to the changes observed for the 4Cu/BEA sample with higher Cu content after poisoning.

3.2.2. NH_3 and NO oxidation

Fig. 5 shows the evolution of NH_3 concentration as a function of the time during NH_3 oxidation (423–773 K) over the fresh and P-poisoned Cu/BEA catalysts. It can be seen in Fig. 5 that both fresh and P-poisoned Cu/BEA catalysts exhibit typical profiles consistent with similar NH_3 oxidation studies reported in the literature [5,10,62].

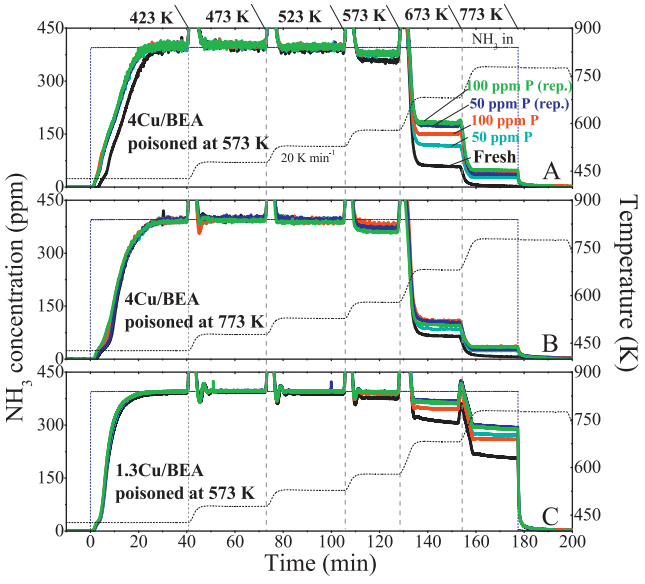

Fig. 5. Evolution of NH_3 concentration as function of the time during NH_3 oxidation (423–773 K) over the fresh and P-poisoned at 573 K (P1) and 773 K (P2) Cu/BEA catalysts after exposure of the samples with 50 and 100 ppm P: 4Cu/BEA (A and B) and 1.3Cu/BEA (C). The reaction studies were performed in the presence of 400 ppm NH_3, 8% O_2 and 5% H_2O.

Accordingly, upon NH_3 admission at 423 K, NH_3 breakthrough appeared, with a steady increase in the exit NH_3 concentration over time, gradually converging to the inlet NH_3 concentration level of 400 ppm. The Cu/BEA catalysts exposed to P exhibit an NH_3 storage at 423 K similar to the data discussed in the previous section, indicating a decreased NH_3 adsorption ability compared with the fresh Cu/BEA samples.

Increasing the temperature up to 573 K does not result in any significant differences in the NH_3 oxidation behaviour in any of the analysed samples. During the transitions from a low temperature to a higher temperature, ammonia desorption peaks were also observed, however these peaks are not fully shown in Fig. 5, in order to present the oxidation behaviour in a more visible manner. In Fig. 5, the later stages of the oxidation at temperatures ≥573 K show significant dissimilarities. NH_3 oxidation occurs over the non-poisoned 4Cu/BEA sample (Fig. 5A) in the range of 573–773 K with a maximum conversion at 773 K, where NH_3 is completely oxidised. The overall process can be described in line with the previous literature [5,10,17,62] and negligible amounts of NO_x and N_2O is formed (data not shown), resulting in that ammonia is mostly oxidised to N_2, according to Eq. (4), as follows:

$$4NH_3 + 3O_2 \rightarrow 2N_2 + 6H_2O \quad (4)$$

On the other hand, the results in Fig. 5A and C clearly show that the NH_3 oxidation at 673 and 773 K is substantially lower over the fresh 1.3Cu/BEA catalyst. This result is in good agreement with our previous study [10], where it was found that the NH_3 oxidation rate per Cu site is significantly higher for the over-exchanged Cu samples.

In contrast to the fresh catalysts, the results in Fig. 5A and C (corresponding to the 4Cu/BEA and 1.3Cu/BEA samples) obtained after P poisoning at 573 K showed a clear poisoning of the NH_3 oxidation. In a similar way, the NH_3 oxidation over the 4Cu/BEA catalysts poisoned at 773 K with 50 and 100 ppm P showed a parallel trend of progressive NH_3 oxidation deterioration (Fig. 5B) with increasing P concentration in the feed. However, the effect is more suppressed in

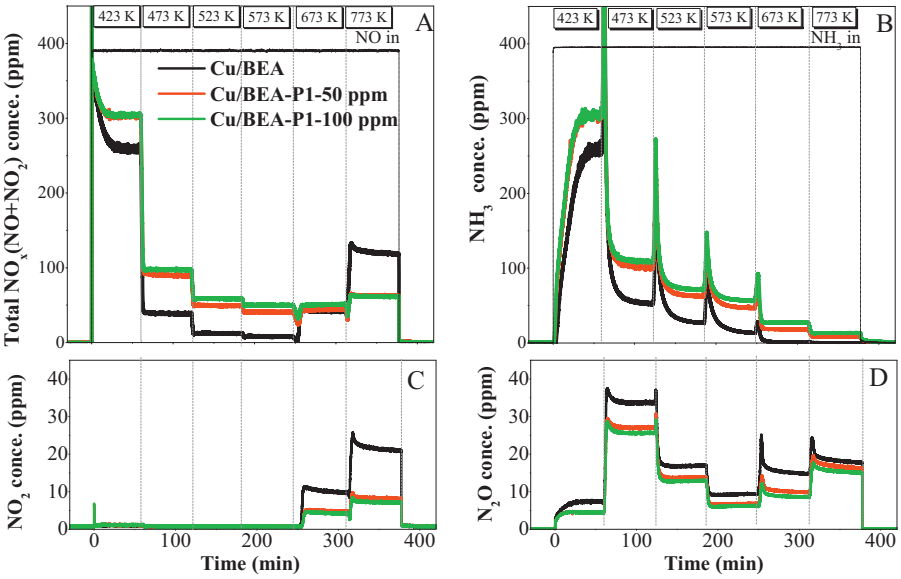

Fig. 6. Evolution of total NO_x (A), NH_3 (B), NO_2 (C) and N_2O (D) of the outlet gas composition during standard NH_3-SCR in the temperature range of 423–773 K over the fresh and P-poisoned at 573 K 4Cu/BEA catalyst after exposure of the sample with 50 and 100 ppm P. The reaction studies were performed in the presence of 400 ppm NO (NH_3), 8% O_2 and 5% H_2O.

comparison to that observed for the 4Cu/BEA–P1 catalysts. Hence, the results clearly show that both parameters of poisoning (temperature and P concentration) are influential in the storage process of NH_3 and its oxidation. The lower temperature of poisoning at 573 K and the presence of P in higher concentrations (100 ppm P) result in the largest decrease in the NH_3 oxidation over Cu/BEA catalysts. This was explained by a partial elimination of the NH_3 adsorption sites due to P deposition on the Cu active sites.

In addition, the repeated experiments of NH_3 oxidation showed that the lowered NH_3 oxidation conversion over the P poisoned catalysts is becoming even further reduced in comparison to that observed after the first NH_3 oxidation experiment. This can be very clearly seen especially for the 4Cu/BEA–P1 sample (Fig. 5A) when the temperature of the reaction is increased to 673 K. This result can be explained by considering that the high temperature treatment of the P poisoned catalysts in the experiments (standard SCR, NO oxidation) before repeating the second test of NH_3 oxidation (see Table 1) has resulted in the migration of condensed H_3PO_4 from the pores of the catalysts to the surface leading to additional P deposition and further elimination of active Cu sites.

The studies carried out over the P-poisoned Cu/BEA catalysts regarding their performance in the reaction of NO oxidation (data not presented) showed that the NO conversion to NO_2 is slightly lower than that observed for the fresh samples. Similar to the studies of NH_3 oxidation, this becomes more obvious with an increase of the temperature to 673 and 773 K where NO oxidation process is more suppressed for the poisoned catalysts while the fresh Cu/BEA catalysts were still able to keep higher NO oxidation activity.

3.2.3. NO_x reduction performance in the reaction of standard NH_3-SCR

Fig. 6 presents the concentration versus time curves for NO_x (A) and NH_3 (B) along with the NO_2 (C) and N_2O (D) in the outlet stream which were used to determine the activity of the fresh 4Cu/BEA catalyst in the reaction of standard NH_3-SCR in the temperature range of 423 – 773 K and its deactivation caused by P poisoning with 50 and 100 ppm P at 573 K. In addition, Fig. 7 displays the percent decrease in the NO_x (Fig. 7A) and NH_3 (Fig. 7B) conversion after P poisoning as a function of the temperature of the reaction. These values were calculated by using the amount of NO_x reduced and NH_3 converted per mol of Cu sites per second over the fresh and P-poisoned catalysts, as described in Section 2. The calculations were carried out for two different 4Cu/BEA catalysts exposed to phosphorous (50 and 100 ppm P) at 573 K and 773 K.

Concerning the results given in Fig. 6, the fresh 4Cu/BEA catalyst exhibits typical NO_x and NH_3 profiles (black curves) consistent with the results reported in our previous study [10] focussed on the effect of Cu loading on the SCR operation of the Cu/BEA catalysts. Accordingly, upon NO and NH_3 admission to the oxygen rich atmosphere at 423 K, the NO_x becomes immediately detectable and reaches a steady state level of about 260 ppm (Fig. 6A). On the other hand, the exit NH_3 concentration (Fig. 6B) steadily increases with time, approaching a concentration level of about 260 ppm after approximately 40 min where the saturation of the sample with NH_3 is almost completely achieved. A further increase in the reaction temperature in the range of 473–573 K increases the activity of the 4Cu/BEA catalyst for NO_x reduction with a maximum NO_x conversion at 573 K. The analysis regarding the products exiting the reactor also showed that the overall reaction has resulted mainly in production of N_2 (estimated based on measured NO, NO_2 and N_2O) accompanied with the formation of small quantities of N_2O. The concentration profiles demonstrating the changes in the NO_x and NH_3 conversion with increasing the temperature up to 573 K showed that the reduction of NO occurs by consuming approximately equimolecular amounts of NH_3 and NO, according to Eq. (5), as follows:

$$4NH_3 + 4NO + O_2 \rightarrow 4N_2 + 6H_2O \quad (5)$$

The analysis of the data for the fresh 4Cu/BEA catalyst at higher temperatures revealed that the NO_x conversion started to decrease with increasing the temperature to 673 and 773 K while the NH_3 conversion shows continuous increase where a maximum NH_3 conversion (100%) is achieved (see Fig. 6A and B). This behaviour was previously explained in the literature [5,18,63–66], by the increased NH_3 oxidation at higher temperatures. Furthermore, in our previous study [10], it was shown that the oxidation rate of NH_3 per Cu site occurs faster over the Cu/BEA catalyst with the higher Cu loading (4 wt% Cu) with respect to the lower Cu content (1.3 wt% Cu).

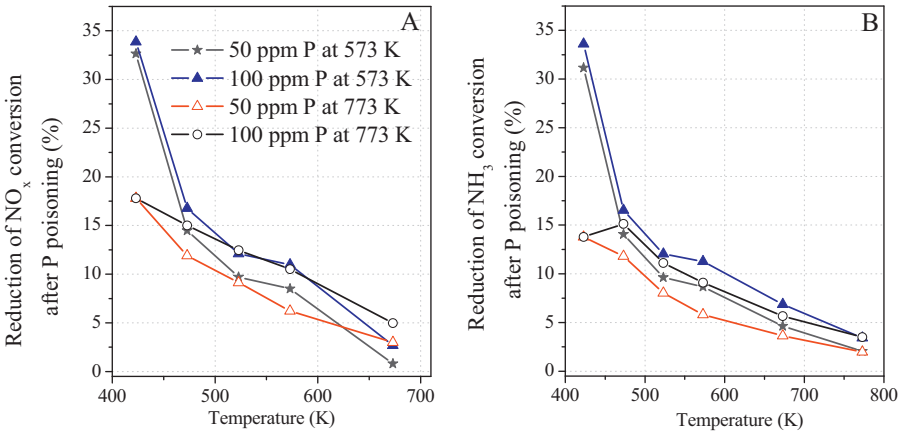

Fig. 7. Reduction of NO_x (A) and NH_3 conversion (B) as function of the temperature (423–673 K) of the reaction of NH_3-SCR over 4Cu/BEA catalyst after exposure of the sample with P at 573 and 773 K.

On the basis of these results, it is apparent that the P-poisoning of the 4Cu/BEA catalyst leads to a visible change in the concentration profiles of total NO_x, NH_3, NO_2 and N_2O (Fig. 6). The NO_x removal performance in comparison to the corresponding fresh sample was decreased, due to poisoning. This can be clearly seen in the whole temperature range of 473–673 K for both 4Cu/BEA samples exposed to 50 and 100 ppm P at 573 K. Our calculations showed a maximum deactivation (~35%) of the 4Cu/BEA catalysts exposed to P at 573 K (Fig. 7A and B) when the reaction of NH_3-SCR was performed at the lowest temperature (423 K). This drastic loss of activity at this temperature is likely related to the changes in the redox-properties of the 4Cu/BEA–P1 catalyst, as discussed earlier, which could be due to blocking of active sites.

Previous studies in the literature [52,67,68] showed that the ability to undergo redox $Cu^{2+} \leftrightarrow Cu^{+}$ cycle is important for the SCR activity and that the redox-active Cu sites are involved in the kinetically relevant step of the SCR reaction. Thus, it can be expected that the formation of phosphate species on the surface probably prohibits the Cu active sites to participate in the $Cu^{2+} \leftrightarrow Cu^{+}$ redox cycle during the SCR reaction. Further, the analysis presented in Fig. 7 showed that the deactivation of the 4Cu/BEA catalyst decreases with increasing the SCR reaction temperature up to 673 K. The decrease in the NO_x and NH_3 conversion after P poisoning of the 4Cu/BEA catalyst (poisoned at 573 K) is about 15% at 473 K, and the deactivation slowly decreases to about 10% at 573 K. Considering that the overall process of reduction of Cu species over the 4Cu/BEA–P1 catalyst is shifted towards higher temperature region, it can be suggested that this partially recovers the loss of activity caused by P with increasing the reaction temperature. Another possible explanation could be desorption/evaporation of the condensed H_3PO_4 acid causing physical blockage of the pore structure at increasing the reaction temperatures.

This behaviour was also observed for the 4Cu/BEA catalyst, P poisoned at 773 K (the data regarding the SCR performance of the sample are not presented) although the deactivation (Fig. 7) was found to be rather limited in comparison to that for the 4Cu/BEA–P1. In particular, this can be clearly seen (Fig. 7) when the SCR measurements were conducted at 423 K for the 4Cu/BEA–P1 catalyst. The 4Cu/BEA–P1 catalyst has a maximum deactivation of ~35%, while the 4Cu/BEA–P2 sample lost only about 16% of its activity. As it was discussed above, the higher temperature of P poisoning of the 4Cu/BEA catalyst at 773 K compared to that at 573 K limits (to some extent) the effect of chemical deactivation of the samples and P deposition on the active Cu sites. In another work, it was shown [31] that once P is present in the gas phase, reactions with O_2 and H_2O may then form H_3PO_4, which may then start condensation reactions and lead to the formation of ultra fine particles. In particular, condensation of these species has been estimated [31] to happen at temperatures lower than 773 K.

Another important aspect regarding the catalytic behaviour of the studied fresh and P-poisoned 4Cu/BEA samples is the difference between the NO_x conversions with increasing the temperature to 773 K. It can be seen in Fig. 6A, that NO_x reduction process by NH_3 occurred on the 4Cu/BEA–P1 catalysts with a higher NO_x conversion and a lower concentration of gaseous NO_x species exiting the reactor compared to the fresh 4Cu/BEA sample. In addition, unreacted NH_3, which is also commonly referred to as NH_3 slip, was detected at 673 and 773 K for the P-poisoned catalysts (about 15 ppm). These results were in good agreement with the data reported in Section 3.2.2 and were found to originate mostly from the lower selectivity towards NH_3 oxidation (Fig. 5A).

In the light of the findings, it can be argued that the P poisoning follows both physical and chemical deactivation and P chemically deactivates Cu/BEA catalysts by changing their redox properties. Furthermore, P deposition occurs mainly on the active Cu species responsible for the catalytic reduction of NO_x by NH_3. It is possible that the pore condensation of H_3PO_4 in combination with pore blocking is the prevailing mechanism in the beginning of the process of P deposition. However, once deposited, P species can also migrate on the surface and partially cover the active Cu sites. In addition, it can be suggested that the accumulated P acts as an effective poison inducing chemical deactivation by reducing the number of the active sites than as impurity blocking the pores of the catalysts.

Further the activity measurements in the reaction of NH_3-SCR were also conducted over the fresh and P-poisoned 1.3Cu/BEA catalysts with significantly lower Cu content (1.3 wt% Cu). These experiments are presented in Fig. 8. As described earlier, the monolith samples were exposed to P with 50 and 100 ppm P at 573 K by changing the concentration of H_3PO_4 in the feed. From the results given in Fig. 8A and B, showing the evolution of total NO_x and NH_3 concentration profiles in the temperature range of 423–773 K, it can be seen that P poisoning did not result in any significant deactivation of the sample even after exposure of the monolith with 100 ppm P at 573 K. The only noteworthy indication regarding the effect of P can be seen when the temperature of the SCR reaction was increased to 773 K at which a higher NO_x reduction activity than the fresh catalytic system was observed.

Based on the data discussed so far, it can be argued that P accumulation on the surface with chemical deactivation occurs preferentially on the so called "*over exchanged*" Cu active sites which are abundant in the 4Cu/BEA sample with the higher Cu loading. This

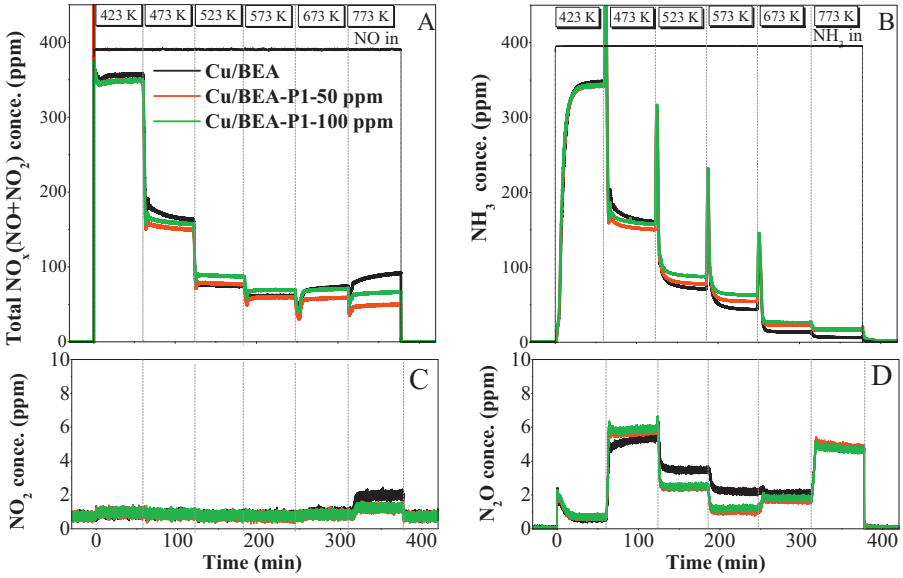

Fig. 8. Evolution of total NO_x (A), NH_3 (B), NO_2 (C) and N_2O (D) of the outlet gas composition during standard NH_3-SCR in the temperature range of 423–773 K over the fresh and P-poisoned at 573 K 1.3Cu/BEA catalyst after exposure of the sample with 50 and 100 ppm P. The reaction studies were performed in the presence of 400 ppm NO (NH_3), 8% O_2 and 5% H_2O.

argument was confirmed by calculating the ratio of the amount of NO_x (in kmol) reduced or NH_3 converted per mol of Cu sites per second. The calculations were performed for various temperatures and the results are plotted in Fig. 9. It should be noted that this is not a rate, since the conversion is high and the plug flow behaviour must be considered for rate calculations. The data in Fig. 9 gives a

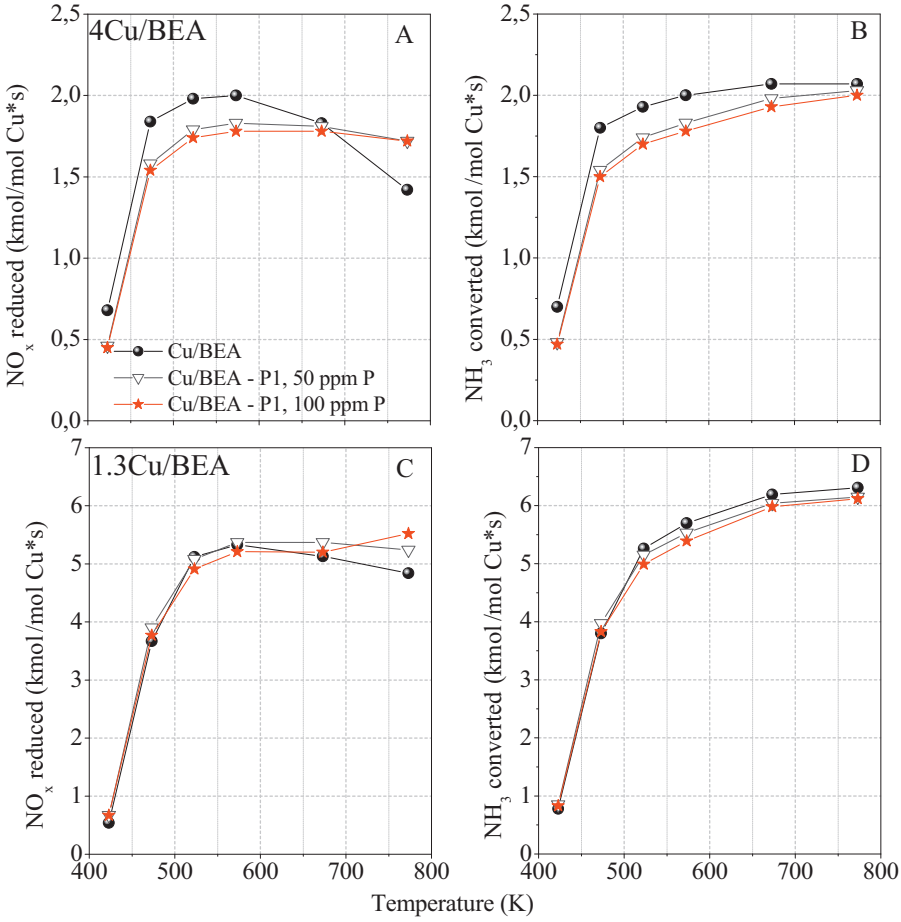

Fig. 9. Estimated amounts of NO_x reduced and NH_3 converted (kmol) per mol Cu active sites per second on the surface during standard NH_3-SCR in the temperature range of 423–773 K over the fresh and P-poisoned 4Cu/BEA (A and B) and 1.3Cu/BEA catalysts (C and D) after exposure of the samples with 50 and 100 ppm P at 573 K.

measure of how the conversion per site is changed in different conditions. However, the amounts of reduced NO_x or converted NH_3 species per mol of Cu sites are more significantly decreased in the case of the 4Cu/BEA sample with the higher Cu content after P poisoning compared to 1.3Cu/BEA. The expected increase in the ratio of the reduced NO_x per mol of Cu sites at 773 K for the P-poisoned catalysts with respect to the corresponding fresh samples, as indicated in Fig. 9, can be attributed to the higher amounts of NH_3 available for the SCR due to the lowered selectivity towards NH_3 oxidation. The reason for this is that the "over-exchanged" Cu sites that are mainly responsible for ammonia oxidation, are more severely poisoned.

4. Conclusions

The effects induced by P over Cu/BEA NH_3-SCR catalysts with different Cu loadings (4 and 1.3 wt% Cu) were studied as a function of the temperature of poisoning and P concentration in the feed. To simulate P poisoning in lean hydrothermal conditions, the monolith catalysts were exposed to different concentrations of P by controlled evaporation of H_3PO_4, in the presence of 8% O_2 and 5% H_2O. The procedure was developed to compare the effects of P poisoning (50 and 100 ppm P) at two different temperatures: 573 and 773 K. The reaction studies involving NH_3-storage/TPD, NH_3/NO oxidation and standard NH_3-SCR were performed in flow reactor experiments in the range of 423–773 K. In addition, a combination of different characterisation techniques (ICP–AES, BET surface area measurements, pore size distribution, H_2-TPR and XPS) was applied to provide useful information regarding the mechanism of P deactivation of the catalysts. Based on these studies, the main conclusions are summarised, as follows:

(a) The poisoning of the Cu/BEA catalysts by P follows both physical and chemical deactivation. It was found that the pore condensation of H_3PO_4 in combination with pore blocking is the mechanism of the process of P deposition, indicating the occurrence of physical deactivation. However, the measured overall deactivation was related mostly to occur due to chemical deactivation by reducing the number of the active Cu sites and hence the redox properties of Cu/BEA catalysts.
(b) It was found that the process of P accumulation on the surface occurs preferentially on the so called "*over exchanged*" Cu active sites with the formation of phosphate species. The higher extent of deactivation of the 4Cu/BEA catalyst than that for the sample with lower Cu content (1.3 wt% Cu) was explained by the presence of "*over exchanged*" Cu active sites which are abundant on the 4Cu/BEA sample.
(c) The P poisoning was found to have a more severe effect when conducted at 573 K compared to that at 773 K. The results clearly showed that the P poisoning at lower temperatures (573 K) has a more significant negative effect on the NH_3 uptake behaviour of the Cu/BEA catalysts due to a partial elimination of the NH_3 adsorption sites on the surface. In addition, the NH_3 oxidation was lowered and also a decrease in the NO_x removal performance in comparison to the corresponding fresh sample over the temperature range of 473–673 K was observed.
(d) A maximum deactivation (of about 35%) of the 4Cu/BEA catalyst exposed to P at 573 K was found to occur when the reaction of NH_3-SCR was performed at the lowest temperature (423 K). On the other hand, at 673 K no significant deactivation was found and even at the higher temperature (773 K) the NO_x reduction performance of the P-poisoned Cu/BEA was increased. The reason for this was found to originate mostly from the lower selectivity towards NH_3 oxidation.

Acknowledgment

This work has been performed at the Competence Centre for Catalysis in collaboration with Combustion Engine Research Centre and Bilkent University in Turkey. We would like to acknowledge the Swedish foundation for strategic research (F06-0006) and Chalmers Initiative Transport, for funding.

References

[1] S. Brandenberger, O. Kröcher, A. Tissler, R. Althoff, Catal. Rev. Sci. Eng. 50 (2008) 492–531.
[2] H. Bosch, F. Janssen, Catal. Today 2 (1988) 369–379.
[3] P. Forzatti, Catal. Today 62 (2000) 51–65.
[4] E. Tronconi, I. Nova, C. Ciardelli, D. Chatterjee, M. Weibel, J. Catal. 245 (2007) 1–10.
[5] H. Sjövall, L. Olsson, E. Fridell, R.J. Blint, Appl. Catal. B: Environ. 64 (2006) 180–188.
[6] R.M. Heck, Catal. Today 53 (1999) 519–523.
[7] C. Ciardelli, I. Nova, E. Tronconi, D. Chatterjee, B. Bandl-Konrad, M. Weibel, B. Krutzsch, Appl. Catal. B: Environ. 70 (2007) 80–90.
[8] H. Sjövall, R.J. Blint, L. Olsson, Appl. Catal. B: Environ. 92 (2009) 138–153.
[9] S. Shwan, J. Jansson, J. Korsgren, L. Olsson, M. Skoglundh, Catal. Today 197 (2012) 24–37.
[10] O. Mihai, C.R.Widyastuti, S., Andonova, K., Kamasamudram, J., Li, S., Joshi, N.W., Currier, A., Yezeretz, L. Olsson, submitted.
[11] R. Nedyalkova, S. Shwan, M. Skoglundh, L. Olsson, Appl. Catal. B: Environ. 138–139 (2013) 373–380.
[12] J.H. Kwak, D. Tran, S.D. Burton, J. Szanyi, J.H. Lee, C.H.F. Peden, J. Catal. 287 (2012) 203–209.
[13] M. Colombo, I. Nova, E. Tronconi, Appl. Catal. B: Environ. 111–112 (2012) 433–444.
[14] M. Wallin, C.-J. Karlsson, M. Skoglundh, A. Palmqvist, J. Catal. 218 (2010) 354–364.
[15] J.H. Kwak, R.G. Tonkyn, D.H. Kim, J. Szanyi, Ch H.F. Peden, J. Catal. 275 (2010) 187–190.
[16] B. Modén, J.M. Donohue, W.E. Cormier, H.X. Li, Stud. Surf. Sci. Catal. 174 (2008) 1219–1222.
[17] M. Colombo, I. Nova, E. Tronconi, Catal. Today 151 (2010) 223–230.
[18] M. Colombo, I. Nova, E. Tronconi, Catal. Today 197 (2012) 243–255.
[19] M. Iwamoto, H. Yahiro, K. Tanda, N. Mizuno, Y. Mine, S. Kagawa, J. Phys. Chem. 95 (1991) 3727–3730.
[20] M.H. Groothaert, J.A. van Bokhoven, A.A. Battiston, B.M. Weckhuysen, R.A. Schoonheydt, J. Am. Chem. Soc. 125 (2003) 7629–7640.
[21] B. Modén, P. Da Costa, B. Fonfé, D.K. Lee, E. Iglesia, J. Catal. 209 (2002) 75–86.
[22] M.Y. Kustova, S.B. Rasmussen, A.L. Kustov, C.H. Christensen, Appl. Catal. B: Environ. 67 (2006) 60–67.
[23] D. Nicosia, I. Czekaj, O. Kröcher, Appl. Catal. B: Environ. 77 (2008) 228–236.
[24] O. Kröcher, M. Elsener, Appl. Catal. B: Environ. 77 (2008) 215–227.
[25] V. Kröger, T. Kanerva, U. Lassi, K. Rahkamaa-Tolonen, M. Vippola, R.L. Keiski, Top. Catal. 45 (2007) 153–157.
[26] V. Kröger, M. Hietikko, U. Lassi, J. Ahola, K. Kallinen, R. Laitinen, R.L. Keiski, Top. Catal. 30/31 (2004) 469–473.
[27] V. Kröger, M. Hietikko, D. Angove, D. French, U. Lassi, A. Suopanki, R. Laitinen, R.L. Keiski, Top. Catal. 42/43 (2007) 409–413.
[28] V. Kröger, T. Kanerva, U. Lassi, K. Rahkamaa-Tolonen, T. Lepistö, R.L. Keiski, Top. Catal. 42/43 (2007) 433–436.
[29] T. Kanerva, V. Kröger, K. Rahkamaa-Tolonen, M. Vippola, T. Lepistö, R.L. Keiski, Top. Catal. 45 (2007) 137–142.
[30] A. Williams, J., Burton, R.L., McCormick, T., Toops, A.A., Wereszczak, E.E., Fo, M.J., Lance, G., Cavataio, D., Dobson, J., Warner, K., Nguyen, D.W. Brookshear, SAE International 2013-01-0513.
[31] F. Castellino, S.B. Rasmussen, A.D. Jensen, J.E. Johnsson, R. Fehrmann, Appl. Catal. B: Environ. 83 (2008) 110–122.
[32] M. Klimczak, P. Kern, T. Heinzelmann, M. Lucas, P. Claus, Appl. Catal. B: Environ. 95 (2010) 39–47.
[33] D.R. Liu, J.-S. Park, Appl. Catal. B: Environ. 2 (1993) 49–70.
[34] M.J. Rokosz, A.E. Chen, C.K. Lowe-Ma, A.V. Kucherov, D. Benson, M.C. Paputa Peck, R.W. McCabe, Appl. Catal. B: Environ. 33 (2001) 205–215.
[35] S.A. Culley, T.F., McDonnell, D.J., Ball, C.W., Kirby, S.W. Hawes (1996) SAE Technical Paper Series 961898: 13-21.
[36] D.D. Beck, J.W. Sommers, C.L. DiMaggio, Appl. Catal. B: Environ. 11 (1997) 257–272.
[37] D.E. Angove, N.W. Cant, Catal. Today 63 (2000) 371–378.
[38] C.C. Webb, G.J.J. Bartley, B.B. Bykowski, G. Fransworth, M. Riley, JSAE 20030269 (2003) 1–12.
[39] G.C. Joy, F.S., Molinaro, E.H. Homeier EH. (1985) SAE Technical Paper Series 852099: 53-64.
[40] R.G. Silver, M.O. Stefanick, B.I. Todd, Catal. Today 136 (2008) 28–33.
[41] D. Nicosia, M. Elsener, O. Kröcher, P. Jansohn, Top. Catal. 42-43 (2007) 333–336.
[42] J.P. Chen, M.A. Buzanowski, R.T. Yang, J. Air Waste Manage. 40 (1990) 1403–1409.
[43] H. Kamata, K. Takahashi, C.U. Obendbrand, Catal. Lett. 53 (1998) 65–71.

[44] J. Beck, R. Muller, J. Brandenstein, B. Matschenko, J. Matschke, S. Unterberger, K.R.G. Hein, Fuel 84 (2005) 1911–1919.
[45] J. Blanco, P. Avila, C. Barthelemy, A. Bahamonde, J.A. Odriozola, J.F. Garcia de la Banda, H. Heinemann, Appl. Catal. B: Environ. 55 (1989) 151–164.
[46] V. Kröger, U. Lassi, K. Kynkäänniemi, A. Suopanki, R.L. Keiski, Chem. Eng. J. 120 (2006) 113–118.
[47] R. Silver, M. Stefanick, B. Todd, Catal. Today 136 (2008) 28–33.
[48] P. Kern, M. Klimczak, T. Heinzelmann, M. Lucas, P. Claus, Appl. Catal. B: Environ. 95 (2010) 48–56.
[49] S. Andonova, V. Marchionni, M. Borelli, R. Nedyalkova, L. Lietti, L. Olsson, Appl. Catal. B: Environ. 132–133 (2013) 266–281.
[50] S. Andonova, V. Marchionni, L. Lietti, L. Olsson, Top. Catal. 56 (2013) 68–74.
[51] G. Centi, S. Perathoner, Appl. Catal. A: Gen. 132 (1995) 179–259.
[52] B. Moden, J.M. Donohue, W.E. Cormier, H.-X. Li, Zeolites and related materials: trends, targets and challenges, in: A. Gédéon, F. Massiani, F. Babonneau (Eds.), Proceedings of 4th International FEZA Conference, Elsevier, 2008.
[53] P. Da Costa, B. Modén, G.D. Meitzner, D.K. Lee, E. Iglesia, Phys. Chem. Chem. Phys. 4 (2002) 4590–4601.
[54] R. Bulánek, B. Wichterlová, Z. Sobalík, J. Tichý, Appl. Catal. B: Environ. 31 (2001) 13–25.
[55] J. Li, N. Wilken, K. Kamasamudram, N.W. Currier, L. Olsson, A. Yezerets, Top. Catal. 56 (2013) 201–204.
[56] M.C. Biesinger, L.W.M. Lau, A.R. Gerson, R.S.C. Smart, Appl. Surf. Sci. 257 (2010) 887–898.
[57] N. Wilken, R. Nedylkova, K. Kamasamudram, J. Li, N.W. Currier, R. Vedaiyan, A. Yezerets, L. Olsson, Top. Catal. 56 (2013) 317–322.
[58] W. Grünert, N.W. Hayes, R.W. Joyner, E.S. Shpiro, M.R.H. Siddiqui, G.N. Baeva, J. Phys. Chem. 98 (1994) 10832–10846.
[59] J.F. Moulder, W.F. Stickle, P.E. Sobol, K.D. Bomben, in: J. Chastain (Ed.), Handbook of X-Ray Photoelectron Spectroscopy, Perkin-Elmer, Eden Prairie, Minnesota, 1992.
[60] Y. Barbaux, M. Dekiouk, D. Le Maguer, L. Gengembre, D. Huchette, J. Grimblot, Appl. Catal. A: Gen. 90 (1992) 51–60.
[61] P.-H. Lo, W.-T. Tsai, J.-T. Lee, M.-P. Hung, Surf. Coat. Technol. 67 (1994) 27–34.
[62] O. Kröcher, M. Devadas, M. Elsener, A. Wokaun, N. Söger, M. Pfeifer, Y. Demel, L. Mussmann, Appl. Catal. B: Environ. 66 (2006) 208.
[63] T. Komatsu, M. Nunokawa, I.S. Moon, T. Takahara, S. Namba, T. Yashima, J. Catal. 148 (1994) 427–437.
[64] H. Sjöval, L. Olsson, R.J. Blint, J. Phys. Chem. C 113 (2009) 1393–1405.
[65] A. Grossale, I. Nova, E. Tronconi, Catal. Today 136 (2008) 18–27.
[66] N. Wilken, K. Wijayanti, K. Kamasamudram, N.W. Currier, R. Vedaiyan, A. Yezerets, L. Olsson, Appl. Catal. B: Environ. 111–112 (2012) 58–66.
[67] S. Kieger, G. Delahay, B. Coq, B. Neveu, J. Catal. 183 (1999) 267–280.
[68] G. Delahay, B. Coq, S. Kieger, B. Neveu, Catal. Today 54 (1999) 431–438.